# Visual Servoing for Non-Holonomic Mobile Robots

Yasuhiro Masutani Masahiko Mikawa Noriaki Maru Fumio Miyazaki

Faculty of Engineering Science, Osaka University
Toyonaka, Osaka 560, Japan

### Abstract

*Although visual servoing is suitable for control of a mobile robot based on a single on-board camera image, wheeled vehicles have a non-holonomic property that the degree of freedom of the input is less than that of the configuration. Thus the visual servoing cannot be directly applied to a camera system fixed on the vehicle. Furthermore there is no smooth and stable state feedback law for non-holonomic vehicle. To overcome these difficulties, we consider another situation that the pan angle of camera is actuated and used as an input of visual servoing. The desired state is given as not a constant value but a trajectory represented in terms of image sequences of a gazed object. Based on this idea, we propose a method of realizing "teaching and playback" for non-holonomic mobile robot. In the teaching mode, the robot gazes a landmark in the environment by a single on-board camera and stores its image sequences while running commanded by a human operator. In the playback mode, the robot tracks the desired trajectory with velocity commands for the vehicle and the pan angle for the camera determined from the stored and current images. We discuss the convergence to a desired state and moreover point out an additional feedback term of a deviation of the pan angle works to improve the tracking performance. The effectiveness of the proposed method is shown by illustrating computer simulation results.*

## 1 Introduction

For wheeled vehicles, dead reckonings of internal sensors is not enough to achieve precise motion control because of slippage. Therefore any usage of external sensors is indispensable to the control of mobile robots. Visual servoing [1][2] is suitable for control of a mobile robot based on an on-board camera image, because it can avoid the dead reckoning problem and reduce a cost to identify the absolute location.

However wheeled vehicles have a non-holonomic property that the degree of freedom of the input (typically linear and angular velocities) is less than that of the configuration (position ($x$, $y$) and orientation $\theta$) [3]. Thus

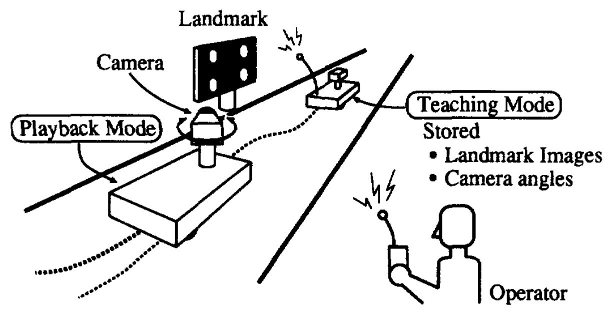


Fig. 1 Teaching and playback of mobile robot by visual servoing

the visual servoing cannot be directly applied to a camera system fixed on the vehicle. Furthermore pure state feedback stabilization around a given terminal configuration is not possible for non-holonomic vehicles [4]. To overcome these difficulties, we considers another situation that the pan angle of camera is actuated and used as an input of visual servoing and that the desired state is given as not a constant value but a trajectory represented in term of image sequences.

Based on the above idea, this paper presents a method to achieve "teaching and playback" for non-holonomic mobile robots (illustrated in Fig. 1). In the teaching mode, the robot gazes a landmark in the environment by panning the on-board camera and stores its image sequences while running commanded by a human operator. In the playback mode, the robot tracks the desired trajectory represented in terms of the stored image sequences with velocity commands for the vehicle and the pan angle for the camera determined from a difference between the stored and current images.

Although visual servoing ensures that the camera configuration in the world coordinate frame converges to a desired trajectory, it is not clear that the vehicle configuration behaves then. We introduce another error system including the hon-holonomic kinematics of the vehicle on the assumption that the deviation of camera orientation is small. If some conditions are satisfied, we can prove that

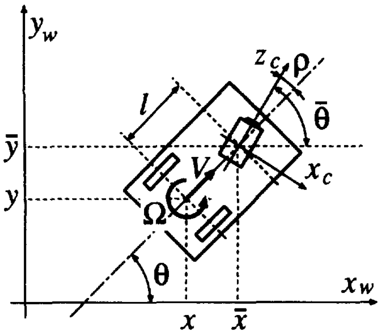


Fig. 2 Model of non-holonomic vehicle with camera

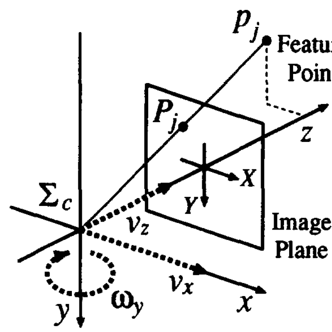


Fig. 3 Model of camera system

the configuration of a mobile robot also converges to the desired trajectory. Moreover we point out an additional feedback term proportional to the deviation of the pan angle has an effect on improving its tracking performance.

In the following sections, first modeling of kinematics of the vehicle and camera is described. Then we present how to construct control input based on the visual servoing concept. Finally results of computer simulation are shown to discuss of the effectiveness of our method. Moreover we apply the method to our actual experimental system.

## 2 Modeling

In this section, we present kinematic models of the vehicle and the camera system.

### 2.1 Vehicle Kinematics

Suppose that the vehicle can move only on a 2D plane and that its configuration is described in position $(x, y)$ and orientation $\theta$ as shown in Fig. 2. The motion of vehicle is controlled by the linear velocity $V$ and the angular velocity $\Omega$. In this paper these velocities are assumed to track a command perfectly. The non-holonomic kinematics of the vehicle is represented as

$$\begin{pmatrix} \dot{x} \\ \dot{y} \\ \dot{\theta} \end{pmatrix} = \begin{pmatrix} \cos\theta & 0 \\ \sin\theta & 0 \\ 0 & 1 \end{pmatrix} \begin{pmatrix} V \\ \Omega \end{pmatrix}. \tag{1}$$

Suppose that a camera is mounted on the vehicle with offset $l$ away from the center of vehicle and can rotate about the vertical axis which goes through the center of lense. For simplicity the optical axis is assumed to be on horizontal plane. The configuration of camera in the world coordinate frame $(\bar{x}\ \bar{y}\ \bar{\theta})$ is expressed by

$$\begin{aligned} \bar{x} &= x + l\cos\theta \\ \bar{y} &= y + l\sin\theta \\ \bar{\theta} &= \theta + \rho \end{aligned} \tag{2}$$

where $\rho$ is the pan angle of the camera relative to the centerline of vehicle. Equations (1) and (2) give the differential relationship between the camera and vehicle displacement of the form

$$\begin{pmatrix} \dot{\bar{x}} \\ \dot{\bar{y}} \\ \dot{\bar{\theta}} \end{pmatrix} = \begin{pmatrix} \cos\theta & -l\sin\theta & 0 \\ \sin\theta & l\cos\theta & 0 \\ 0 & 1 & 1 \end{pmatrix} \begin{pmatrix} V \\ \Omega \\ \dot{\rho} \end{pmatrix}. \tag{3}$$

### 2.2 Camera Kinematics

Fig. 3 shows a camera model we use. Let the possible motion of the camera be described as velocity $\boldsymbol{u} = (v_x\ v_z\ \omega_y)$ in the camera coordinate frame $\Sigma_C$. In this paper we consider that the landmark consists of $n$ feature points. Let $\boldsymbol{p}_j = (x_j\ y_j\ z_j)^T$ be the $j$th feature point in $\Sigma_C$ and $\boldsymbol{P}_j = (X_j\ Y_j)^T$ be the corresponding projection on the image plane. Then the velocity of feature point on the image $\dot{\boldsymbol{P}}_j$ is written by

$$\dot{\boldsymbol{P}}_j = \boldsymbol{L}_j^T \boldsymbol{u} \tag{4}$$

where $\boldsymbol{L}_j^T$ is the image Jacobian matrix for $j$th point defined by

$$\boldsymbol{L}_j^T = \begin{pmatrix} -f/z_j & X_j/z_j & -f - X_j^2/f \\ 0 & Y_j/z_j & -X_jY_j/f \end{pmatrix} \tag{5}$$

where $f$ is the focal length. By combining all feature points, we obtain the following relationship.

$$\dot{\boldsymbol{P}} = \boldsymbol{L}^T \boldsymbol{u} \tag{6}$$

where

$$\boldsymbol{P} = (\boldsymbol{P}_1^T\ \boldsymbol{P}_2^T \cdots \boldsymbol{P}_n^T)^T \in R^{2n} \tag{7}$$

$$\boldsymbol{L}^T = (\boldsymbol{L}_1\ \boldsymbol{L}_2 \cdots \boldsymbol{L}_n)^T \in R^{2n\times 3}. \tag{8}$$

## 3 Control Method

### 3.1 Visual Servoing

First we define a task function by the current and desired (reference) images of the feature points as follows

$$e = C(\boldsymbol{P} - \boldsymbol{P}_d) \tag{9}$$

where $C \in R^{3\times 2n}$ is a certain matrix which stabilizes the system and $\boldsymbol{P}_d(t)$ is memorized in the teaching mode. By differentiating $\boldsymbol{e}$, we obtain an error system

$$\begin{aligned} \dot{\boldsymbol{e}} &= C(\dot{\boldsymbol{P}} - \dot{\boldsymbol{P}}_d) + \dot{C}(\boldsymbol{P} - \boldsymbol{P}_d) && (10)\\ &= CL^T\boldsymbol{u} - C\dot{\boldsymbol{P}}_d + \dot{C}(\boldsymbol{P} - \boldsymbol{P}_d). && (11)\end{aligned}$$

Then feedback law is in the form

$$\boldsymbol{u} = -\lambda e + (L^T)^+\dot{\boldsymbol{P}}_d + (\dot{L}^T)^+(\boldsymbol{P} - \boldsymbol{P}_d) \tag{12}$$

where $\lambda$ is a positive scalar gain and we use pseudo-inverse matrix of the image Jacobian for $C$

$$C = (L^T)^+. \tag{13}$$

Therefore the error system is rewritten as

$$\dot{\boldsymbol{e}} = -\lambda \boldsymbol{e} \tag{14}$$

which means the function $\boldsymbol{e}$ converges zero while $t \to \infty$. As a result the camera configuration is converges to the desired state if the velocity is perfectly controlled by equation (12).

### 3.2 Control input to the vehicle

Transformation of the velocity from the camera frame to the world frame is expressed by

$$\begin{pmatrix} \dot{\bar{x}} \\ \dot{\bar{y}} \\ \dot{\bar{\theta}} \end{pmatrix} = \begin{pmatrix} \sin\bar{\theta} & \cos\bar{\theta} & 0 \\ -\cos\bar{\theta} & \sin\bar{\theta} & 0 \\ 0 & 0 & -1 \end{pmatrix} \begin{pmatrix} v_x \\ v_z \\ \omega_y \end{pmatrix}. \tag{15}$$

Substituting it to the inverse of equation (3) yields the following form

$$\boldsymbol{U} = T(\rho)\boldsymbol{u}, \tag{16}$$

where $\boldsymbol{U} = (V\ \Omega\ \dot{\rho})^T$ and

$$T(\rho) = \begin{pmatrix} \sin\rho & \cos\rho & 0 \\ -(\cos\rho)/l & (\sin\rho)/l & 0 \\ (\cos\rho)/l & -(\sin\rho)/l & -1 \end{pmatrix}. \tag{17}$$

The command of velocity for the vehicle and pan angle is determined by this relation.

### 3.3 Convergence of the orientation $\theta$

When the camera configuration converges to a desired state by the feedback law mentioned above, how does the vehicle configuration behave? If the $\boldsymbol{e}$ is small enough, we can consider $\boldsymbol{e}$ as a deviation of position and orientation in the camera frame;

$$\boldsymbol{e} = \begin{pmatrix} \sin\bar{\theta} & -\cos\bar{\theta} & 0 \\ \cos\bar{\theta} & \sin\bar{\theta} & 0 \\ 0 & 0 & -1 \end{pmatrix} \begin{pmatrix} \bar{x} - \bar{x}_d \\ \bar{y} - \bar{y}_d \\ \bar{\theta} - \bar{\theta}_d \end{pmatrix}. \tag{18}$$

Under this assumption, combining the equations (3), (12), (16), and (18) yields the error system for $\boldsymbol{\xi} = (\boldsymbol{e}^T\ \ \theta - \theta_d) \in R^4$ of the following form

$$\dot{\boldsymbol{\xi}} = \boldsymbol{f}(\boldsymbol{\xi}, \boldsymbol{U}_d(t)). \tag{19}$$

This model includes the non-holonomic kinematics of the vehicle. By using Liapunov method, if a condition

$$V_d > 0, \quad |\Omega_d| < \alpha V_d / l \tag{20}$$

is satisfied for the desired trajectory, the stability of $\boldsymbol{\xi} = \boldsymbol{o}$ in a region

$$|\theta - \theta_d| < \pi - 2\tan^{-1}\alpha \tag{21}$$

is assured where $\alpha$ is a certain positive constant.

### 3.4 Improvement of Tracking Performance

Some results of computer simulation show that the tracking performance at the center of vehicle is not fast enough. Therefore we improve the control input by using the following $\boldsymbol{u}'$ instead of $\boldsymbol{u}$

$$\boldsymbol{u}' = \boldsymbol{u} + \begin{pmatrix} \cos\rho_d \\ -\sin\rho_d \\ 0 \end{pmatrix} k\{\rho - \rho_d - h(\dot{\rho} - \dot{\rho}_d)\} \tag{22}$$

where $k$ and $h$ are positive constants. The additional term is proportional to the deviation of pan angle and is effective in only the velocity inputs $v_x$ and $v_z$. Moreover its direction is nearly orthogonal to the desired orientation of the vehicle if $|\theta - \theta_d|$ is small. It is similar to a way by human driver to steer a large car (bus or truck). In case that this improvement is applied, the pan angle is also stored in the teaching mode.

Constants $k$ and $h$ must be chosen so that the stability is kept. Linearizing the system (19) with an additional input of (22) and checking the eigenvalues, we can conclude that if a condition

$$k < l\lambda + V_d, \quad h > 0 \tag{23}$$

is satisfied, the linearized system is stable. In addition, we have to choose these constants by taking notice that there are a delay and a noise in the process of detecting $\dot{\rho}$.

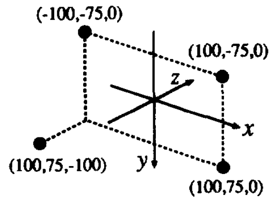


Fig. 4 Feature Points (Landmark)

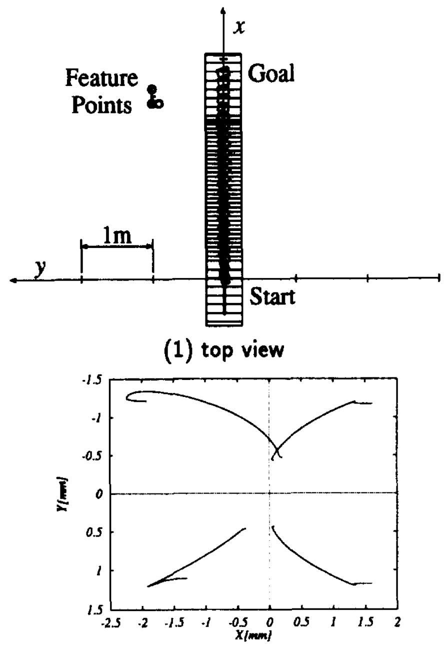


(1) top view

(2) loci of feature points on the image plane

Fig. 5 Desired trajectory given in the teaching mode

## 4 Simulation

We verify the effectiveness of the proposed method through the computer simulation.

### 4.1 Conditions

Suppose that the landmark consists of 4 feature points as shown in Fig. 4 whose relative location is known. Therefore the depth of points can be computed from the feature images $P_1, \cdots, P_4$. The landmark and camera is 750mm high from the floor. We assume that the correspondence of feature points between the desired and current image is known. In the initial state, the optical axis of the camera is in the direction of the landmark.

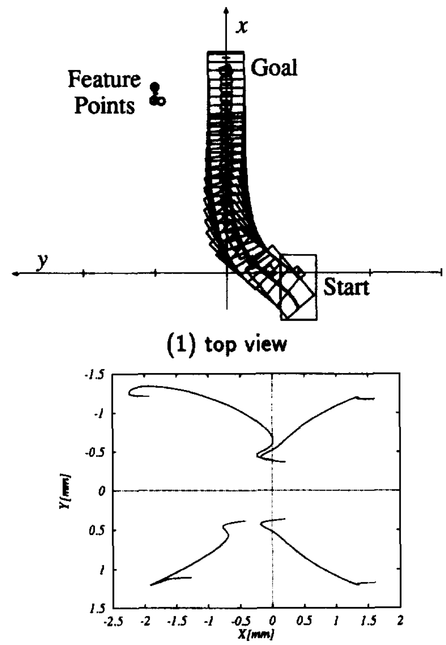


(1) top view

(2) loci of feature points on the image plane

Fig. 6 Playback with initial position error ($k = 0$)

Each parameter is that focal length $f = 16$(mm), offset of camera from the vehicle center $l = 480$(mm), sampling time is 33(msec), gain $\lambda = 1$, and $h = 1$. Time derivatives of $(L^T)^+$, $\boldsymbol{P}$, and $\rho$ are computed from a difference of the sampling value.

### 4.2 Teaching

Fig. 5 shows the desired trajectory in a top view and the plot of feature points on the image plane which are given by a human operation in the teaching mode. The velocity $V_d = 200$(mm/sec) except for the accelerative and declarative section and $\Omega_d = 0$.

### 4.3 Playback with Initial Position Error

First we present a results of playback with a initial position error 1000(mm) in $y$ direction in Fig. 6 for $k = 0$, Fig. 7 for $k = 0.5l$ and Fig. 8 for time plot of the variable.

The trajectory of the vehicle center for $k = 0.5l$ converges the desired trajectory faster than that for $k = 0$. Fig. 8 also shows that the errors for $k = 0.5l$ vanish faster.

Fig. 9 shows the trajectory of vehicle center for various $k$.

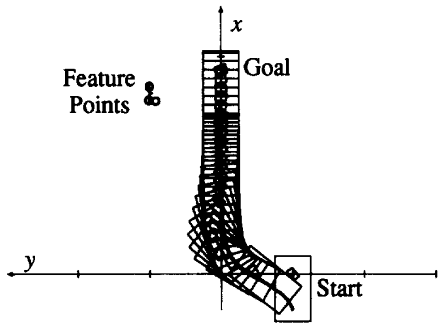


(1) top view

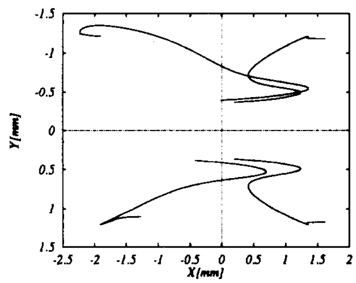


(2) loci of feature points on the image plane

Fig. 7 Playback with initial position error ($k = 0.5l$)

### 4.4 Playback with Initial Orientation Error

Next a results of playback with a initial orientation error 90(degree) are shown in Fig. 10 for $k = 0$, Fig. 11 for $k = 0.5l$ and Fig. 12 for time plot of the variable.

In these simulations the initial error of the camera configuration is zero. In case of $k = 0$ the error is kept zero while controlling. On the other hand, In case of $k = 0.5l$ the error of camera increases in the early time by the disturbance of additional term but the error of vehicle vanish faster than the case $k = 0$.

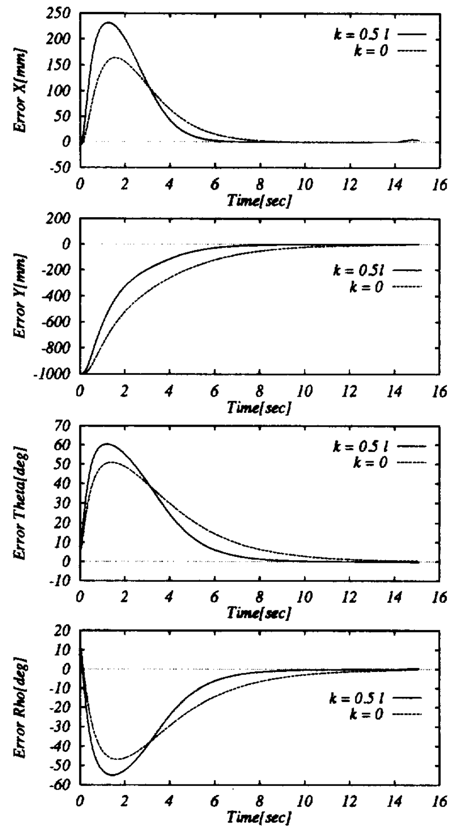


Fig. 8 Time plot of the errors with intial position error

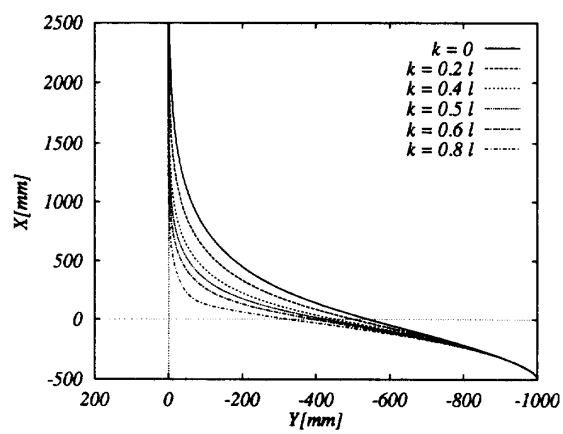


Fig. 9 Playback trajectories for various $k$

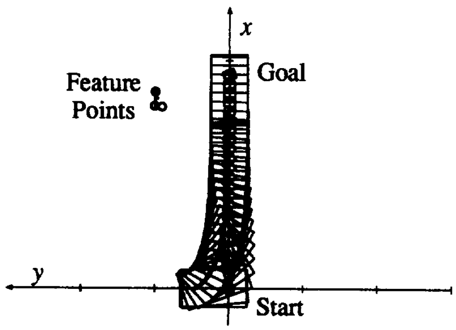


(1) top view

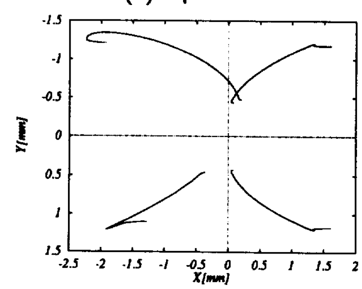


(2) loci of feature points on the image plane

Fig. 10 Playback with initial orientation error ($k = 0$)

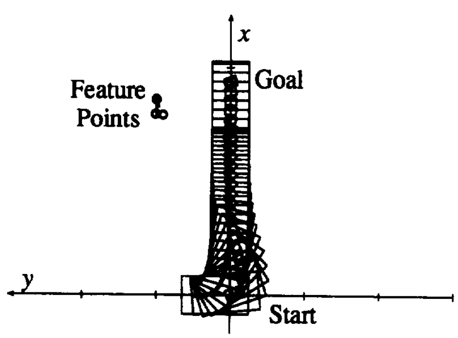


(1) top view

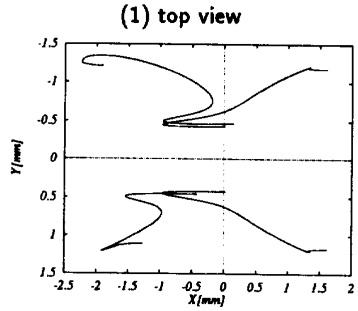


(2) loci of feature points on the image plane

Fig. 11 Playback with initial orientation error ($k = 0.5I$)

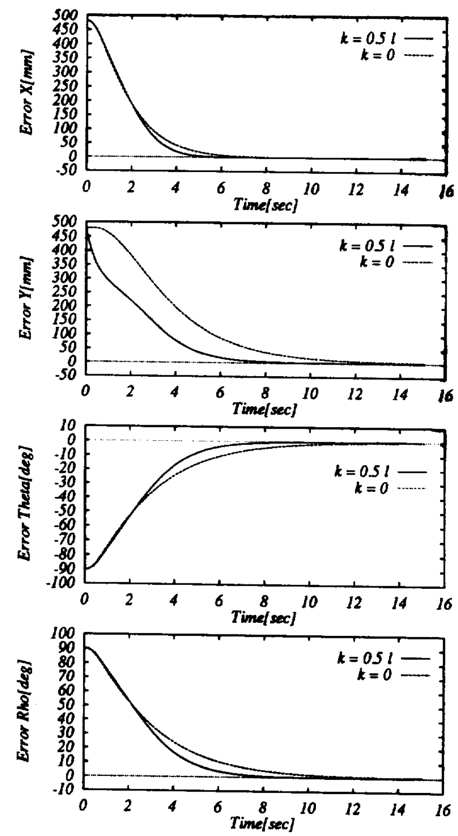


Fig. 12 Time plot of the errors with initial orientation error

## 5 Experiment

We apply the proposed method to our 3-wheeled mobile robot system. This system consists of a body of parts transporter (wheel base: 480 mm), a camera (focal length: 16 mm) whose pan angle can be actuated by a DC motor, analog servoing circuits, two Transputers (T805, 25MHz) for image processing and computation of the command, and a personal computer (8086, 5MHz) for the communication with operator as shown in Fig. 13. A Landmark is made of 4 white disks on a black board. Images taken by the camera are converted to binary and digitized in 256×240 pixels and stored every 66 msec.

An example of performance by using the method (12) is shown in Fig. 14 ~ Fig. 16. Fig. 14 shows loci of feature points on the image plane in the teaching and playback modes. Fig. 15 and Fig. 16 show the position and orientation $(x, y, \theta)$ of robot in the world frame which is calculated from the image taken by another camera on the ceiling which is not used for the control. The result demonstrates that the proposed method enables non-holonomic mobile robots to navigate by visual servoing without the dead reckonings of internal sensors. The performance is not much better than the simulation because of the hardware limitation, that is, the friction of camera drive system and the quantization error of image.

## 6 Conclusion

In this paper, we present the feedback control method to realize teaching and playback of non-holonomic mobile robots. By adding the pan angle of camera to the input we can apply the idea of visual servoing to the control of camera motion mounted on the non-holonomic vehicle.

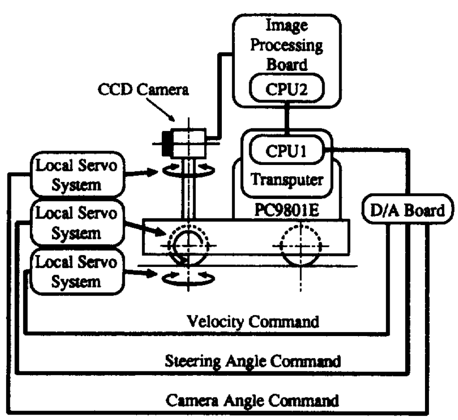


Fig. 13 Experimental System

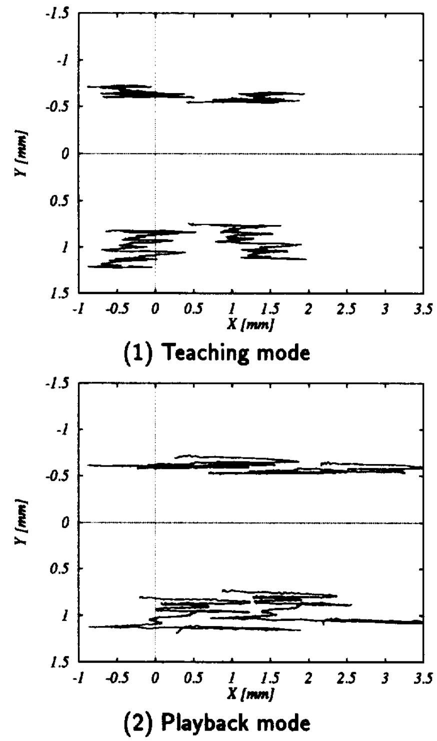


Fig. 14 Loci of feature points on the image plane in the teaching and playback modes (experiment)

Then the configuration of vehicle converges to a desired state simultaneously. Furthermore an additional feedback term of the deviation pan angle improves the tracking performance of the vehicle.

We are planning to use a binocular camera system [5] which enables us to avoid the assumption of the knowledge about the feature points.

## References


[1] Arthur C. Sanderson Lee E. Weiss and Charles P. Neuman. Dynamic sensor-based control of robots with visual feedback. *IEEE Journal of Robotics and Automation*, 3(5):404–417, 1987.

[2] Bernard Espiau, François Chaumette, and Patrick Rivers. A new approach to visual servoing in robotics. *IEEE Transaction on Robotics and Automation*, 8(3):313–326, 1992.

[3] Yutaka Kanayama, Yoshihiko Kimura, Fumio Miyazaki, and Tesuo Noguchi. A stable tracking control method for an autonomous mobile robot. In

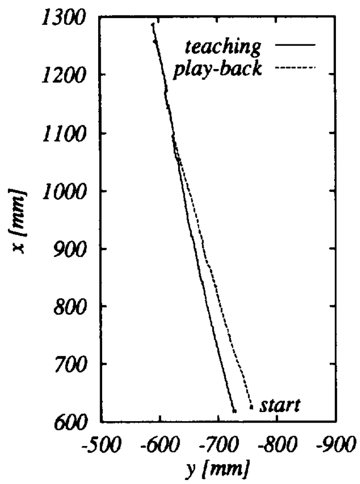


**Fig. 15 Paths of the robot in the top view in the teaching and playback modes (experiment)**


*Proc. IEEE Int. Conf. on Robotics and Automation*, Cincinnati, U.S.A., 1990.

[4] Claude Samson and Karim Ait-Abderrahim. Feedback control of nonholonomic wheeled cart in cartesian space. In *Proc. IEEE Int. Conf. on Robotics and Automation*, Sacramento, U.S.A., 1991.

[5] Noriaki Maru, Hiroshi Kase, Atsushi Nishikawa, Shinya Yamada, and Fumio Miyazaki. Manipulator control by visual servoing with the stereo vision. In *Proc. IEEE/RSJ Int. Conf. on Intelligent Robots and Systems '93*, Yokohama, Japan, 1993.


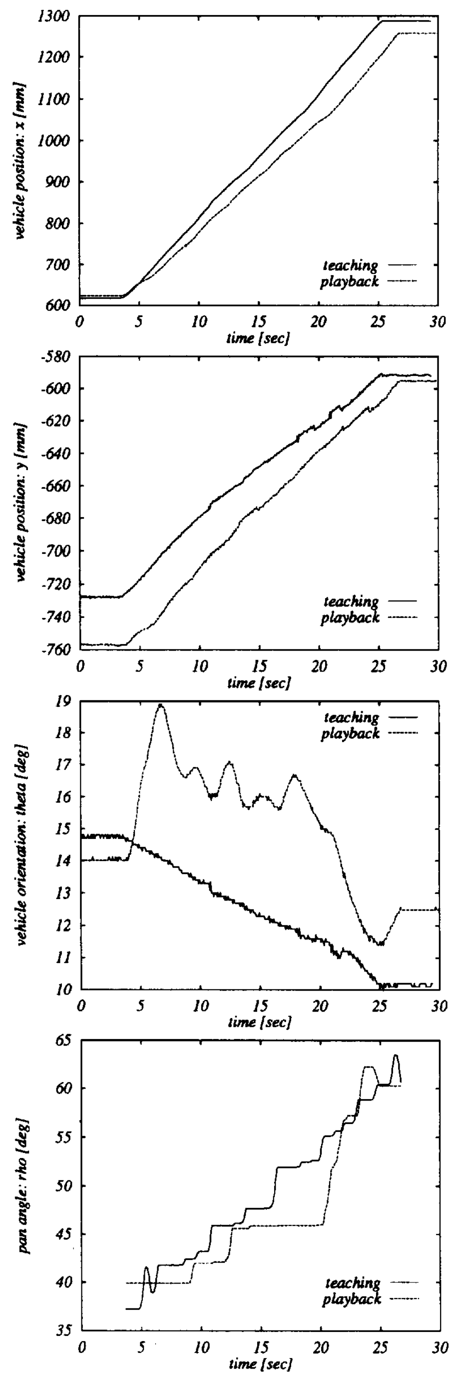


**Fig. 16 Time plot of position and orientation of the robot (experiment)**